Theory and Simulation of the Beam Cyclotron Instability

M. LAMPE, W. M. MANHEIMER, J. B. MCBRIDE, J. H. ORENS, K. PAPADOPOULOS, R. SHANNY, AND R. N. SUDAN*
U. S. Naval Research Laboratory, Washington, D. C. 20390

(Received 5 August 1971)

A detailed theory in conjunction with the results of computer simulation experiments is presented for the beam cyclotron instability. The main results are (1) After a period of exponential quasilinear development, turbulent wave-particle interactions cause cross-field diffusion of the electrons which smears out the electron gyroresonances. This occurs at a level of turbulence which scales as $\Sigma_k(|E_k|^2/4\pi N_0 T_e) \sim (\Omega_e/\omega_e)^2(\Omega_e/kv_e)$, where Ω_e and ω_e are the electron cyclotron and plasma frequencies, and results in a transition to ordinary ion sound modes that would occur in an unmagnetized plasma. The magnetic field serves to reduce the effects of electron trapping. (2) This level of turbulence appears to have virtually no effect on long wavelength fluid modes. (3) At this level the instability stabilizes if ordinary ion sound is stable due to ion Landau damping. For cold ions it continues to develop at the slower ion acoustic growth rate until the fields become strong enough to trap the ions. After the fields saturate, further plasma heating is much slower than exponential.

I. INTRODUCTION

Recently, there has been considerable interest in the theory of electrostatic plasma instabilities that are driven by the relative streaming of electrons and ions across a magnetic field.[1–10] These studies have been motivated in part by the need to determine the mechanisms responsible for turbulent heating seen in cross-field magnetosonic shock waves (most recently reported in Ref. 11 for $T_e \lesssim T_i$ and in Ref. 12 for $T_e \gg T_i$) and in theta-pinch experiments.[10] The nonzero value of curl **B** in shock fronts and magnetic pistons indicates the presence of a cross-field current, which may be driven by the **E**×**B** drift or by drifts due to gradients in density, temperature, or magnetic field.

The first such instability to be studied was the Buneman two-stream instability,[1] which occurs when $v_d > v_e$ and $kr_e < 1$, and which quickly heats the electrons to $v_e \sim v_d$. [Here, v_d is the electron–ion relative drift speed, $v_e \equiv (T_e/m_e)^{1/2}$ is the electron thermal speed, $r_e \equiv v_e/\Omega_e$ is the typical electron gyroradius, and Ω_e is the electron cyclotron frequency.] However, Sagdeev[2] pointed out the importance of slower instabilities which continue to heat the plasma when $v_d \lesssim v_e$. Subsequently, Krall and Book[3] discussed a class of low-frequency ion acoustic instabilities driven by density and magnetic field gradients, with $\omega < \Omega_e$ in the electron frame.

This paper presents a comprehensive linear and nonlinear theory (supported by computer simulation) of a class of faster-growing high-frequency instabilities with $kr_e > 1$ which we shall call the beam cyclotron instability. These instabilities are due to the coupling of electron Bernstein modes to ion beam modes, and are driven principally by the **E**×**B** drifts.[13] The linear theory of the beam cyclotron instability has been discussed by Wong,[4] Gary and Sanderson,[5] Lashmore-Davies,[6] Forslund, *et al.*,[7] and Lampe, *et al.*[8] The fact that the instability persists when ion temperature T_i exceeds T_e was first pointed out in Ref. 6, and the existence of the instability was confirmed by computer experiments in Ref. 7. The first theory of the nonlinear development of this instability has recently been presented in a preliminary letter by the present authors[9] which also reports computer simulations in excellent agreement with the theory. In this paper we present a summary, including important new results, of linear theory, and we discuss the mechanisms governing nonlinear development in full detail, i.e., quasilinear diffusion, turbulent broadening of the electron gyroresonances, and ion trapping.

In Sec. IIA we discuss the consequences of the linear dispersion relation. It is assumed that the time scale of interest is long compared with Ω_e^{-1} but short compared with the ion gyroperiod Ω_i^{-1}, so that the ions are unmagnetized, and the model of a homogeneous system with an electron–ion relative drift is adopted. The instability occurs in discrete bands of wavenumber or frequency, each band associated with a particular electron cyclotron harmonic. For the case of cold ions and for v_d/v_e small, the maximum growth rate occurs for $k \simeq 1/\sqrt{2}\lambda_D$ and is of order $(m_e/m_i)^{1/4}(\Omega_e \omega_e v_d/v_e)^{1/2}$, as first shown in Ref. 4, where λ_D is the electron Debye length, m_e/m_i is the electron–ion mass ratio, and ω_e is the electron plasma frequency. The location and width of the unstable bands is given, as is the dependence of ω on k. A very useful simplified dispersion relation is derived under the weak assumption $kr_e > 1$; in this form, the usual infinite sum of Bessel functions is replaced by a closed expression.

A theorem of general interest in linear theory, first presented as a conjecture in Ref. 8, is proven. The theorem states that under certain conditions (in particular, for the beam cyclotron instability, that $T_i = 0$), $\int dk\, \gamma_k$ with the integral taken over the *unstable modes only* is independent of the magnetic field. This is indicative of the fact that the introduction of the external magnetic field into linear theory distorts the existing ion-acoustic instability, quantizing it into discrete bands, but without mixing the unstable branch with any damped branch of the dispersion relation. In either of the two limits, $B \to 0$ or $v_d \gg v_e$, the bands coalesce and the instability spectrum becomes continuous.

In Sec. IIB we argue, following Dum and Dupree,[14] that in the presence of turbulent electric fields resulting from the instability, an electron no longer has a well-defined gyro-orbit—there is now a component of cross-field spatial diffusion. When the diffusion coefficient D, which is proportional to the field energy $\langle E^2\rangle$, is calculated, and is fed back into the zero-order electron orbits, a dispersion relation nonlinear in the wave amplitudes is obtained. In fact, this nonlinear dispersion relation is of the same form as the linear dispersion relation discussed in Sec. IIA, except that the electron gyroresonances are broadened by a frequency $\Delta\omega_k = k^2D$, i.e., by the inverse of the time necessary for an electron to diffuse a distance of the order of the wavelength. When $\Delta\omega_k \ll \Omega_e/\pi$, diffusion becomes unimportant and linear theory prevails. But when the turbulent fields are so strong that $\Delta\omega_k \gtrsim \Omega_e/\pi$, the electrons are essentially untied from the field lines over distances and times characteristic of the beam-cyclotron instability, and the magnetic field is easily seen to drop out of the dispersion relation. What remains is the dispersion relation appropriate to the ion acoustic instability in a magnetic-field-free plasma. Thus, at a certain level of turbulence, a transition is made from the beam-cyclotron instability to the ion acoustic instability. However, the magnetic field plays the important role of preventing long time electron trapping in the usual sense. This level scales as $\sum_k |E_k|^2/4\pi N_0 T_e \sim (\Omega_e/\omega_e)^2 \times (1/kr_e)$, where N_0 is the electron number density. If $\Omega_e/\omega_e \ll 1$, as is true in many shock experiments,[11,12] this transition occurs at a very low level of turbulence.

In Sec. III we discuss the quasilinear development of the electron and ion temperatures. There are two distinct stages of quasilinear development: the beam cyclotron instability, for low levels of turbulence, and later the ion acoustic instability. We find that if $T_i \ll T_e$, in both stages the energy extracted from the streaming motion is partitioned so that the electrostatic energy, ion temperature, and electron temperature all grow exponentially, with growth rates in the ratio 5:3:2. However, the coefficients are such that most of the energy goes into electron heating, and very little into the fields. The difference between the two stages is only that the growth rate is considerably faster for the beam-cyclotron than for the ion acoustic instability.

When the waves become big enough to trap ions, in our computer experiments we find that the instability saturates. By using the condition $2e\phi = \frac{1}{2}m_i(v_d - \omega/k)^2$ for ion trapping,[15] and also using the quasilinear equation for T_e, we estimate that the electron temperature at saturation is $T_e \sim 0.02 m_i v_d^2$. Following ion trapping, continued plasma heating is observed. This heating is linear rather than exponential, however.

For the case of warm ions, on the other hand, it is important to note that ion acoustic waves may be stable, as a result of ion Landau damping, although beam-cyclotron modes are unstable. A rough criterion for ion sound stability, valid for a hydrogen plasma in the range $0.1 \lesssim (T_i/T_e,\ v_d/v_e) \lesssim 1$, is $T_i/T_e > v_d/v_e$. If T_i/T_e exceeds this requirement, the transition from beam-cyclotron to ion acoustic waves results in stabilization. As observed, this nonlinear stabilization can occur at a rather early stage, for conditions prevailing in many shock experiments.

To summarize then, one important result of Secs. II and III is that the instability can be stabilized in any of three different ways: (1) Linearly. The growth rate decreases for $k > 2^{-1/2}\lambda_D^{-1}$. The minimum unstable value of k (corresponding to the fundamental frequency Ω_e) is $k \approx \Omega_e/v_d$. Thus, if $(v_e/v_d) > 2^{-1/2}\omega_e/\Omega_e$, the growth rate decreases as the electrons heat further, growth is no longer exponential, and rapid heating ceases. (2) Resonance broadening. If T_i/T_e is too large, roughly if $T_i/T_e \gtrsim v_d/v_e$, the transition to ion acoustic waves, as a result of turbulent diffusion, kills the instability. (3) Ion trapping. Whichever of these conditions occurs first, depending on the particular experimental parameters, will terminate the instability.

In Sec. IV we observe that in some systems the beam cyclotron instability can exist simultaneously with other instabilities. For example, Papadopoulos, *et al.*[16] have discussed a two-stream instability of cross-field counterstreaming ion beams, with long wavelength, $kr_e \sim (m_e/m_i)^{1/2} \ll 1$, which occurs only because the electrons are tied down to the field lines. The question then arises, will the turbulent diffusion resulting from the beam cyclotron instability stabilize such long-wavelength instabilities by untieing the electrons from the field lines? We find that this cannot happen. Electron diffusion over distances as long as the ion–ion wavelength would require turbulent electric fields far larger than those generated by the beam cyclotron instability.

In Sec. V, we present results of extensive numerical experiments, confirming all the main points of the theory. Much of the nonlinear theory of the instability presented in this paper was motivated by the initial computer experiments.

Section VI contains a summary of the results, and their implications for perpendicular shock waves.

II. DISPERSION RELATION

A. Linear Theory

We consider electrostatic waves driven unstable by the relative streaming of electrons and ions across a uniform magnetic field **B**. The linear dispersion relation can immediately be written as

$$\epsilon(\mathbf{k}, \omega) \equiv 1 + \mu_i(\mathbf{k}, \omega) + \mu_e(\mathbf{k}, \omega) = 0, \qquad (1)$$

where μ_e and μ_i are the susceptibilities contributed by the electrons and ions, respectively. In this paper we shall confine our attention to situations where the ions are unaffected by the magnetic field, i.e., the time scale of all processes both linear and nonlinear is much

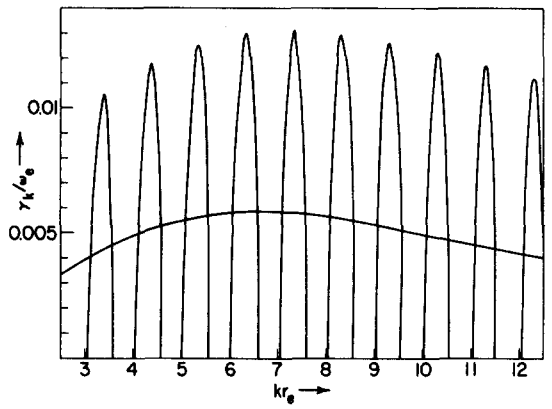

FIG. 1. Growth rate vs wavenumber for a hydrogen plasma with $v_d/v_e=1$, $T_i/T_e=0$ for the cases $\Omega_e/\omega_e=0.1$, $\Omega_e=0$ (smooth curve).

shorter than an ion gyroperiod. Within this limitation, in a reference frame in which the ions drift with velocity v_d with respect to the electrons, μ_e and μ_i are given by

$$\mu_i=-(2k^2\lambda_D^2)^{-1}(T_e/T_i)Z'[(\omega-\mathbf{k}\cdot\mathbf{v}_d)/\sqrt{2}kv_i], \quad (2)$$

$$\mu_e=-\frac{\omega_e^2}{k^2}\int d^3\mathbf{v}\left[1-\sum_{n=-\infty}^{\infty}\frac{\omega}{\omega-n\Omega_e}J_n^2\left(\frac{kv_\perp}{\Omega_e}\right)\right]v_\perp^{-1}\frac{\partial f_e}{\partial v_\perp}, \quad (3)$$

where $k\equiv|\mathbf{k}|$, $v_\perp\equiv|\mathbf{v}-(\mathbf{v}\cdot\mathbf{B})(\mathbf{B}/B^2)|$ is the velocity normal to $\mathbf{B}$, $v_i\equiv(T_i/m_i)^{1/2}$ is the ion thermal speed, f_e is the electron velocity distribution, and Z' is the derivative of the plasma dispersion function.

We shall, for the most part, be interested in the short-wavelength region of the unstable wave spectrum, i.e., $kr_e>1$. In this limit it is possible to sum all the harmonics appearing in μ_e. Following the procedure detailed by Coppi, *et al.*,[17] which is summarized in Appendix A, we obtain the following expression for μ_e:

$$\mu_e=(k^2\lambda_D^2)^{-1}+(k^2\lambda_D^2)^{-1}\frac{\omega}{2\sqrt{2}kv_e}\left\{Z\left(\frac{\omega}{\sqrt{2}kv_e}\right)-Z\left(-\frac{\omega}{\sqrt{2}kv_e}\right)+i\cot\left(\pi\frac{\omega}{\Omega_e}\right)\left[Z\left(\frac{\omega}{\sqrt{2}kv_e}\right)+Z\left(-\frac{\omega}{\sqrt{2}kv_e}\right)\right]\right\}. \quad (4)$$

Notice that in this version of μ_e the magnetic field appears only in the cotangent term, which will be of great use later in displaying certain properties of this dispersion relation. The dispersion relation with μ_e in the form given by (4) is especially suited to numerical computation, and we have evaluated the growth rate γ_k and the real frequency ω_k for a wide range of plasma parameters. Figure 1 furnishes an example for a hydrogen plasma with $\omega_e/\Omega_e=10$, $v_d/v_e=1$, and $T_i/T_e=0$.

In order to understand the nature of the computer solutions, we now consider a particular limit[8] that is physically significant and yields simple expressions for ω_k and γ_k. In this limit, which is characterized by $T_i\ll T_e$ and

$$\omega/\sqrt{2}kv_e\approx 2^{-1/2}v_d/v_e\ll 1, \quad (5)$$

we obtain[18]

$$1+k^2\lambda_D^2-[k^2c_s^2/(\omega-kv_d)^2]=(\tfrac{1}{2}\pi)^{1/2}(\omega/kv_e)\cot[\pi(\omega/\Omega_e)], \quad (6)$$

where $c_s=(T_e/m_i)^{1/2}$ is the ion sound speed. Writing $\omega_k=n\Omega_e+\delta_k$ and assuming

$$\gamma_k,\ \delta_k\ll\Omega_e/\pi,\ |\ n\Omega_e-kv_d\ |, \quad (7)$$

it is easy to show that

$$\omega_k-kv_d\simeq -kc_s(1+k^2\lambda_D^2)^{-1/2}-\delta_k, \quad (8a)$$

$$\gamma_k^2=(m_e/8\pi m_i)^{1/2}n\Omega_e^2(1+k^2\lambda_D^2)^{-3/2}-\delta_k^2. \quad (8b)$$

Wong treated this special case in the limit $\delta_k=0$. From Eq. (8a) it is evident that the modes have essentially the phase velocity of ion sound when viewed from the ion frame. The cotangent term on the right-hand side of the dispersion relation (6) serves to generate the Bernstein modes near $n\Omega_e$. Hence, in the electron reference frame we may regard the Bernstein modes as coupled to ion sound and driven unstable by the "ion beam." Notice however that for $k\lambda_D<1$ the group velocity is one-half the phase velocity, whereas in the absence of the magnetic field both of these velocities are equal.

Equations (8) show that the unstable modes occur in discrete bands in k space. These bands are centered on the cyclotron harmonics, $\omega_k=n\Omega_e$, $k=n\Omega_e/[v_d-c_s/(1+k^2\lambda_D^2)^{1/2}]$ and have bandwidths given by

$$\delta\omega\simeq 2\gamma_k(\delta_k=0) \quad (9a)$$

and

$$\delta k\simeq 2\delta\omega/v_d. \quad (9b)$$

The restriction of the unstable modes to narrow bands must be taken into account in computer simulations of this instability where only a limited number of discrete modes are available to the system. Equation (9b) has been simplified by assuming $v_d\gg c_s$; in the opposite case $v_d<c_s$, Eqs. (8a) and (8b) are still valid but the growth rates are feeble. Assumption (7) requires that

$$v_e/v_d>[\Omega_e/(8\pi)^{1/2}\omega_i][1/k\lambda_D(1+k^2\lambda_D^2)^{1/2}], \quad (10)$$

where ω_i is the ion plasma frequency.

The fastest growing instability band is the one that falls closest to

$$k_0\equiv 1/(\sqrt{2}\lambda_D), \quad (11a)$$

which corresponds to the harmonic number nearest to

$$n_0=2^{-1/2}(v_d/v_e)(\omega_e/\Omega_e). \quad (11b)$$

For $k>k_0$, the growth rate falls off as k^{-1}. Thus rapid heating as a result of this instability can occur only if $n_0\geq 1$. This establishes an upper bound on v_e, and also indicates that if $v_e>v_d$ (the situation of interest), then ω_e/Ω_e must be greater than unity.

Numerical solutions of the dispersion relation using expression (4) for μ_e agree very well with the solutions (8a) and (8b) provided the limitations (5) and (10) are observed. For v_d/v_e too large to satisfy (5) and (10), numerical solutions with $T_i=0$ show that the growth rate maxima become larger than those predicted by (8b). When the inequality (10) fails badly, the unstable bands are somewhat widened and shifted away from the cyclotron harmonics toward higher frequencies. In the limit opposite to (10), the nth instability band begins at ω just below $n\Omega_e$ and k just above $n\Omega_e/v_d$. When $v_d/v_e \gtrsim 3$, for a hydrogen plasma, the bands overlap and the unstable spectrum approaches the smooth curve of the usual two-stream instability. In the limit $B\to 0$ and $\Omega_e<\gamma_k$, the magnetic field disappears from (4) because $\cot\omega/\Omega_e\to -i$ and the instability goes over continuously to the field free situation. This indicates that the magnetic field does not create a totally new instability but rather quantizes the unstable spectrum into discrete bands. The maximum growth rates can be enhanced several times over their $B=0$ values but the unstable region of k space becomes correspondingly reduced (see Fig. 1), so as to conserve the area under the γ_k-k curve. Indeed we can prove a remarkable theorem to this effect.

Theorem: If $T_i=0$, the quantity

$$Q\equiv \int_{-\infty}^{\infty} dk\, \gamma_k,$$

where the integral is taken over the unstable modes only (i.e., $\gamma_k>0$) is independent of the magnetic field.

The proof of this theorem follows from expressing Q in the form

$$Q=\int_{-\infty}^{\infty}\frac{dk}{2\pi i}\,\mathrm{Im}\int_C d\omega\,\frac{\omega}{\epsilon(k,\omega)}\,\frac{\partial}{\partial\omega}\epsilon(k,\omega), \qquad (12)$$

where C is the contour (shown in Fig. 2) enclosing all roots of the exact dispersion relation $\epsilon(k,\omega)=0$ with $\mathrm{Im}\omega>0$. The semicircle at infinity does not contribute since $(\omega/\epsilon)(\partial\epsilon/\partial\omega)\sim\omega^{-2}$ as $|\omega|\to\infty$. The order of integration is now reversed giving

$$Q=\mathrm{Im}\int_{-\infty+i\delta}^{\infty+i\delta}\frac{d\omega}{2\pi i}\,\omega\int_{-\infty}^{\infty}\frac{dk}{\epsilon}\,\frac{\partial\epsilon}{\partial\omega}. \qquad (13)$$

If

$$\int_{-\infty}^{\infty}\frac{dk}{\epsilon}\,\frac{\partial\epsilon}{\partial\omega}$$

is an analytic function of ω in the upper half plane, then the ω contour can be moved to $i\infty$. As $\mathrm{Im}\omega\to\infty$, $(1/\epsilon)\partial\epsilon/\partial\omega$ becomes independent of B. Thus, Q is independent of B. The subtleties connected with the legitimacy of the steps taken in the formal proof are discussed in Appendix B. The proof is strictly valid for $T_i=0$.

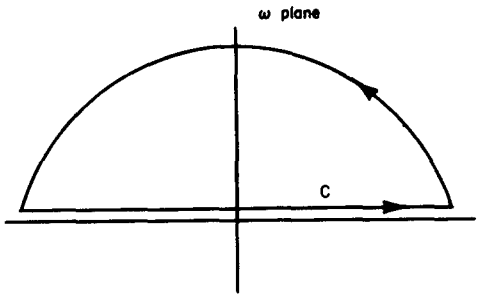

FIG. 2. Contour of integration corresponding to Eq. (B3).

Electromagnetic Effects: In order to justify the assumption of electrostatic modes, the calculation was repeated, using the full set of Maxwell's equations. The resulting linear dispersion relation decouples into a purely electromagnetic mode and a mixed mode. In the limit $c\to\infty$, the electrostatic case, Eq. (1), is recovered from the mixed mode. For the restrictions under which (8a) and (8b) are valid, it can be shown that the most restrictive conditions for neglecting the self-consistent magnetic field ($v_d\ll c$) are

$$\frac{v_e v_d}{c^2}\ll\left(\frac{8\pi m_e}{m_i}\right)^{1/2}\left(\frac{\omega_e}{\Omega_e}\right)^3\frac{(k\lambda_D)^5}{(1+k^2\lambda_D^2)^{3/2}} \qquad (14a)$$

and

$$\frac{v_e^{3/2}v_d^{1/2}}{c^2}\lesssim\left(\frac{m_e}{m_i}\right)^{1/4}\left(\frac{\omega_e}{\Omega_e}\right)^{1/2}\frac{(k\lambda_D)^{5/2}}{(1+k^2\lambda_D^2)^{3/4}}. \qquad (14b)$$

If $\omega_e/\Omega_e\gtrsim 3$, then (14b) is more restrictive than (14a) for the important modes $k\lambda_D\sim 2^{-1/2}$.

Case $T_e\sim T_i$: The linear theory for the case $T_e\sim T_i$ has been discussed earlier in Refs. 6 and 7. The main result is that it is possible to have a resonant instability corresponding to the beam-cyclotron instability in situations where the usual ion acoustic instability for $B=0$ would be stable. The numerical analysis of Forslund *et al.*[7] shows that, in fact, linear growth rates are relatively insensitive to T_i/T_e, decreasing somewhat in passing from the algebraic ($T_i/T_e\ll 1$) to the resonant situation ($T_i\gtrsim T_e$).

This case is somewhat different in detail from the case $T_i\ll T_e$. For example, the most unstable wave has $\omega/k=v_d-v_i$ rather than v_d-c_s, the instability bands can widely overlap in k while remaining distinct in ω, and for $k\lambda_D>1$, the growth rates decrease as $(k\lambda_D)^{-4}$, rather than as $(k\lambda_D)^{-1}$.

B. Nonlinear Theory

When the wave amplitudes of the unstable spectrum become large enough to perturb the electron orbits, then the linear dispersion relation requires some modification. With reasonable justification one may assume the wave spectrum to be randomly phased, so that the

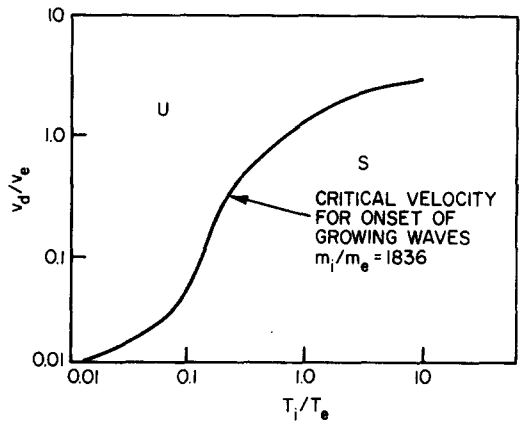

FIG. 3. Stability boundary as given by Stringer (Ref. 20) for a hydrogen plasma. The region U is unstable, while the region S is stable.

random motion of the electrons in such fields can be described in terms of a diffusion. This results in a broadening of wave-particle resonances, as postulated by Dupree[19] which is dependent on the field amplitudes. Thus, we may write

$$\mu_e^{\mathrm{NL}} = -\frac{\omega_e^2}{k^2}\int d^3\mathbf{v}\left[1-\sum_{n=-\infty}^{\infty}\frac{\omega J_n^2(kv_\perp/\Omega_e)}{\omega-n\Omega_e+i\Delta\omega_k}\right]v_\perp{}^{-1}\frac{\partial f_e}{\partial v_\perp}, \tag{15}$$

where $\Delta\omega_k \equiv k^2 D$ is the resonance-broadening term, D being the cross-field spatial diffusion coefficient. A theory for $\Delta\omega_k$ has been developed by Dum and Dupree[14] for an isotropic wave spectrum. We adopt their expression for $\Delta\omega_k$ but modify it to a one-dimensional wave spectrum. Specifically, since the diffusion of electron guiding centers is normal to $\mathbf{k}$, the first term on the right-hand side of Eq. (56) of Ref. 14 vanishes. The remaining terms arise from velocity diffusion, which is proportional to a random component of the gyroradius and azimuthal position. Thus we obtain

$$\Delta\omega_k = \frac{1}{4}\frac{e^2}{m_e{}^2}\frac{k^2}{\Omega_e{}^2}\sum_{k'}\sum_n |E_{k'}|^2\left[J_{n+1}{}^2\left(\frac{k'v_\perp}{\Omega_e}\right)+J_{n-1}{}^2\left(\frac{k'v_\perp}{\Omega_e}\right)\right] \times \frac{\Delta\omega_{k'}+\gamma_{k'}}{(\omega_{k'}-n\Omega_e)^2+(\Delta\omega_{k'}+\gamma_{k'})^2}. \tag{16}$$

We now assume that the electrons retain their Maxwellian distribution during the development of the instability. This is justified by numerous computer experiments to be described in Sec. V. Then, following the procedure used in obtaining (4), and approximating $\Delta\omega_k(v_\perp)$ by $\langle\Delta\omega_k\rangle = \int d^3v\, f_e \Delta\omega_k(v_\perp)$ in (15), we obtain the nonlinear version of (4):

$$\mu_e^{\mathrm{NL}} = (k^2\lambda_D{}^2)^{-1}+(k^2\lambda_D{}^2)^{-1}(\omega/2\sqrt{2}kv_e)\,(Z(\zeta)-Z(-\zeta) +i\cot\{\pi[(\omega+i\langle\Delta\omega_k\rangle)/\Omega_e]\}[Z(\zeta)+Z(-\zeta)]), \tag{17}$$

where $\zeta \equiv (\omega+i\langle\Delta\omega_k\rangle)/\sqrt{2}kv_e$. In a similar manner it is possible to sum the harmonics in the expression for $\Delta\omega_k$ and we obtain,

$$\frac{\langle\Delta\omega_k\rangle}{\Omega_e} = (8\sqrt{2})^{-1}\frac{\omega_e{}^2}{\Omega_e{}^2}\frac{kv_e}{\Omega_e}\sum_{k'}\frac{|E_{k'}|^2}{4\pi N_0 T_e}\frac{k}{k'} \times \mathrm{Im}[G(\zeta_+)+G(\zeta_-)], \tag{18a}$$

where

$$G(\zeta_\pm) = Z(\zeta_\pm)-Z(-\zeta_\pm)+i\cot\{\pi[(\omega+i\langle\Delta\omega_{k'}\rangle)/\Omega_e]\} \times[Z(\zeta_\pm)+Z(-\zeta_\pm)] \tag{18b}$$

and

$$\zeta_\pm = (\omega\pm\Omega_e+i\langle\Delta\omega_{k'}\rangle)/\sqrt{2}k'v_e. \tag{19}$$

The quantity μ_e^{NL} depends on Ω_e directly through the cotangent, and indirectly through $\Delta\omega_k$ [Eq. (18)] which occurs both in the cotangent and in ζ. If $\langle\Delta\omega_k\rangle/\sqrt{2}kv_e$ is small, and can be neglected in ζ, then μ_e^{NL} depends on B only through the cotangent. A case where $\langle\Delta\omega_k\rangle/\sqrt{2}kv_e$ is not negligible in ζ, will be noted in Sec. V. Retaining this term serves to reduce the growth rate.

The linear theory developed in the previous section is recovered in the limit $\pi\langle\Delta\omega_k\rangle/\Omega_e \ll 1$ and $\langle\Delta\omega_k\rangle \lesssim \gamma_k$. For $\Omega_e/\pi \gg \langle\Delta\omega_k\rangle \gtrsim \gamma_k$, the growth rates are reduced somewhat from their linear values. In this case, and for $T_i \ll T_e$, Eq. (8a) is virtually unaltered, but (8b) now reads

$$(\gamma_k+\langle\Delta\omega_k\rangle)^2 = (m_e/8\pi m_i)^{1/2}n\Omega_e{}^2(1+k^2\lambda_D{}^2)^{-3/2} \times[1+(\langle\Delta\omega_k\rangle/\gamma_k)]-\delta_k{}^2. \tag{20}$$

Strong Turbulence: At a level of turbulence such that $\langle\Delta\omega_k\rangle/\Omega_e \gtrsim 1/\pi$, the cotangent term in (17) is approximately $-i$ and we arrive at the important result that the nonlinear dispersion relation goes over to the linear dispersion relation in the absence of a magnetic field. For $|\omega/\sqrt{2}kv_e| < 1$, this transition is to the ion acoustic instability, which is unstable only in the region shown graphically in Fig. 3[20] (for a hydrogen plasma). We note that, in the regime $0.1 \lesssim (T_i/T_e, v_d/v_e) \lesssim 1$, a rough criterion for the existence of an instability is $T_i/T_e < v_d/v_e$.

For the case of cold ions, the solution to the dispersion relation in this regime is given by

$$\omega_k - kv_d \simeq -kc_s(1+k^2\lambda_D{}^2)^{-1/2}, \tag{21}$$

$$\gamma_k \simeq [\tfrac{1}{8}\pi(m_e/m_i)]^{1/2}kv_d(1+k^2\lambda_D{}^2)^{-3/2}. \tag{22}$$

The critical amplitude of the turbulent fields for this transition is obtained by setting $\langle\Delta\omega_k\rangle/\Omega_e = 1/\pi$. From the expression (18) for $\langle\Delta\omega_k\rangle$ we obtain, after replacing the cotangent by $-i$ wherever it appears,

$$\sum_{k'}\frac{|E_{k'}|^2}{4\pi N_0 T_e}\frac{k}{k'} = \left(\frac{2}{\pi}\right)^{3/2}\frac{\Omega_e{}^2}{\omega_e{}^2}\frac{\Omega_e}{kv_e}. \tag{23}$$

At this amplitude it may be argued that most of the electrons would get trapped and hence stabilize the system. However, longtime trapping in a large amplitude coherent wave, in the usual sense, is ruled out by the presence of even a weak magnetic field which serves to untrap the electrons.

In their treatment of the saturation of high-frequency ion cyclotron flute modes of a mirror confined plasma, Dum and Sudan[21] arrived at a similar expression for the critical fields for ion gyroresonance broadening. The ion cyclotron modes actually stabilize at these critical fields but in the case of electron-cyclotron modes such a stabilization only takes place if T_i/T_e is too large for an ordinary ion acoustic instability. In the opposite situation the waves still continue to grow but at the reduced growth rate given by (22). The ultimate saturation of these modes is discussed in Sec. III.

The transition to a nonmagnetic instability occurs more readily for higher harmonics. When $T_i \sim T_e$, all harmonics with $k\lambda_D \lesssim 1$, $kv_e/\Omega_e \gg 1$ have about the same growth rate; thus, the appropriate value of k to use in the transition condition (23) is $k_{\min}=\Omega_e/v_d$. For a peaked spectrum, which is the case when $T_e \gg T_i$, the appropriate value of k is that corresponding to the fastest growing modes, which contribute most, i.e., $k \sim \lambda_D^{-1} \sim k'$.

It is well to note that in many perpendicular shock experiments[11] where $\Omega_e/\omega_e \ll 1$, T_i/T_e is too large for an ordinary ion acoustic instability. Thus, if the ion distribution in these experiments is Maxwellian, they fall in the stable region of Fig. 3, and stabilization of the initially unstable modes will occur at a low level of turbulence. Thus, the main region of interest for the beam cyclotron instability, assuming Maxwellian ions, is for situations where $T_i < T_e$.

III. QUASILINEAR THEORY

We now go on to discuss the quasilinear evolution of the plasma. Specifically, we derive rate equations for v_d, T_e, and T_i in terms of the fluctuating fields. The field energy evolves according to

$$\frac{d}{dt} \mid E_k \mid^2 = 2\gamma_k(v_d, T_e, T_i) \mid E_k \mid^2, \tag{24}$$

where we have indicated the explicit dependence of γ_k on v_d, T_e, and T_i. γ_k may be given either by Eq. (8b) or (22) depending on the stage of the instability. The equations for v_d and T_i can be obtained from the ion quasilinear equation

$$\frac{\partial f_i}{\partial t} = \frac{2e^2}{m_i^2} \sum_k k^2 \mid \Phi_k \mid^2 \frac{\partial}{\partial v} \frac{\gamma_k}{(\omega_k - kv)^2 + \gamma_k^2} \frac{\partial f_i}{\partial v}, \tag{25}$$

where $\mid E_k \mid^2 \equiv k^2 \mid \Phi_k \mid^2$ and the sums are over positive k. The frequency and growth rate are determined from the dispersion relation discussed in the previous section.

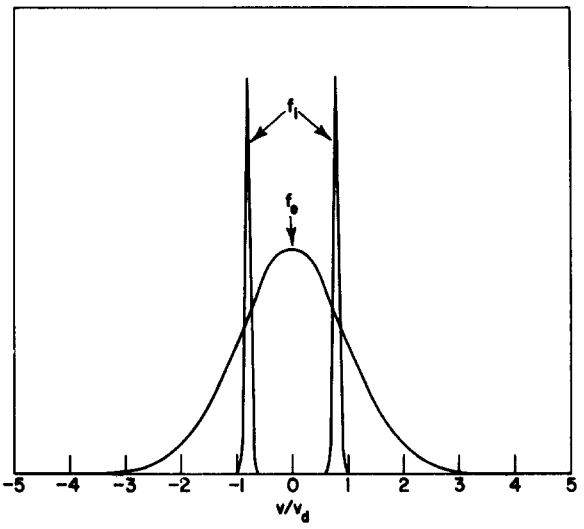

FIG. 4. Cold ion beams counterstreaming normal to **B** through Maxwellian electrons.

Taking appropriate moments of Eq. (25) and assuming that $T_i/T_e \ll 1$, $v_d/v_e \lesssim 1$ yields

$$\frac{dT_i}{dt} = \frac{2e^2}{m_i} \sum_k k^2 \left(\frac{k^2 c_s^2}{1+k^2\lambda_D^2} + \gamma_k^2 \right)^{-1} \frac{d}{dt} \mid \Phi_k \mid^2 \tag{26}$$

and

$$\frac{dv_d}{dt} = \frac{-2e^2}{m_i} \sum_k k^4 c_s (1+k^2\lambda_D^2)^{-1/2} \times \left(\frac{k^2 c_s^2}{1+k^2\lambda_D^2} + \gamma_k^2 \right)^{-2} \frac{d}{dt} \mid \Phi_k \mid^2. \tag{27}$$

The electron quasilinear equation may be written as

$$\frac{\partial f_e}{\partial t} = \mathrm{Re} \sum_k 2 \frac{e}{m_e} \frac{\partial}{\partial \mathbf{v}} \cdot \langle \mathbf{E}_{-k} f_{ke} \rangle, \tag{28}$$

where the summation is over positive k and where the linear expression for f_{ke} is used. Then an expression for the change of electron temperature is

$$\begin{aligned} \frac{dT_e}{dt} &= \sum_k \int d^3\mathbf{v}\, e v_\perp^2 \frac{\partial}{\partial \mathbf{v}} \cdot \langle \mathbf{E}_{-k} f_{ke} \rangle \\ &= -\sum_k \int d^3\mathbf{v}\, 2e\mathbf{v} \cdot \langle \mathbf{E}_{-k} f_{ke} \rangle \\ &= -\sum_k 2\langle \mathbf{E}_{-k} \cdot \mathbf{J}_{ke} \rangle, \end{aligned} \tag{29}$$

$\mathbf{J}_{ke}$ being the electron component of the total current at wavenumber k. Rather than evaluating the right-hand side of Eq. (29) directly, we invoke Poynting's theorem which states

$$\left\langle E_{-k} \frac{\partial}{\partial t} E_k \right\rangle + 4\pi \langle E_{-k} J_{ke} \rangle + 4\pi \langle E_{-k} J_{ki} \rangle = 0. \tag{30}$$

The last term is simply 4π times the rate of change of

TABLE I. Each column refers to a different numerical experiment. Rows 1–4 give basic experimental parameters. Rows 5–7 refer to the beam cyclotron phase: harmonic number of the largest amplitude mode, measured growth rate, and maximum theoretical growth rate. Rows 8 and 9 give the measured level of turbulence at the "knee", and the theoretical value, Eq. (23). Rows 10 and 11 give the measured growth rate in the acoustic phase and the maximum theoretical ion acoustic growth rate. Rows 12–14 give the measured value of $k_{tr}\lambda_D$ (k_{tr} is the wavenumber of the trapping mode), and the measured and theoretical [Eq. (37)] values of $T_e/m_iv_d^2$ at the onset of ion trapping.

	Run number						
	1	2	3	4	5	6	7
(1) m_i/m_e	1 836	1 836	1 836	1 836	400	400	400
(2) Ω_e/ω_e	0.1	0.2	0.2	0.4	0.1	0.2	0.4
(3) System size	512	1 024	512	512	512	512	512
(4) No. particles	140 000	140 000	100 000	140 000	140 000	100 000	140 000
(5) Harmonic No.	beam-cyclotron	2	2	1	5	2	1
(6) $\gamma_{M,\,cyc}/\omega_e$	instability	0.0056	0.0071	0.017	0.010	0.013	0.025
(7) $\gamma_{th,\,cyc}/\omega_e$	not seen	0.015	0.016	0.022	0.020	0.026	0.036
(8) $E^2/4\pi N_0T_e\,\vert_M$	not seen	0.012	0.017	0.06	0.002 to 0.004	0.011	0.07
(9) $E^2/4\pi N_0T_e\,\vert_{th}$	0.0017 (in thermal noise)	0.007	0.010	0.07	0.0013	0.011	0.07
(10) $\gamma_{M,\,sound}/\omega_e$	0.0033	0.0017	0.0012	0.00074	0.0071	0.0056	0.0014
(11) $\gamma_{th,\,sound}/\omega_e$	0.0025	0.0022	0.0022	0.0025	0.0096	0.0060	0.0054
(12) $k_{tr}\lambda_D$	not run to saturation	1.1	0.88	1.3	0.78	0.72	1.3
(13) $T_e/m_iv_D^2\,\vert_M$		0.008	0.012	0.0056	0.04	0.025	0.025
(14) $T_e/m_iv_D^2\,\vert_{th}$		0.005	0.010	0.0019	0.015	0.019	0.002

total ion energy, so that Eq. (30) simply states conservation of particle plus electrostatic energy density. It is now clear that $\Delta\omega_k$ can be interpreted as an anomalous electron–electron collision frequency, since it does not directly affect the rate equation for ion drift, ion temperature, and electron temperature. Therefore, there can be no anomalous heating or resistivity resulting directly from this $\Delta\omega_k$. Using Eqs. (26), (27), and (30), the quasilinear equation for electron temperature is

$$\frac{dT_e}{dt} = -\frac{1}{2}\frac{dT_i}{dt} - m_iv_d\frac{dv_d}{dt} - \sum_k (4\pi N_0)^{-1}\frac{d}{dt}\mid E_k\mid^2. \quad (31)$$

Comparing terms in Eq. (31), we find that the contribution $m_i\,v_d\,(dv_d/dt)$ is dominant as long as $v_d \gg c_s$. Thus, most of the energy coupled out of the beam goes to heating electrons and we may write

$$T_e(t) - T_e(0) \approx \tfrac{1}{2}m_i[v_d^2(0) - v_d^2(t)]. \quad (32)$$

Due to the large ion mass, a small change in beam velocity gives a substantial change in electron temperature. Using Eq. (27) for v_d, we may immediately write

$$\frac{dT_e}{dt} = \frac{2e^2m_i^{1/2}v_d}{T_e^{3/2}}\sum_k (1+k^2\lambda_D^2)^{3/2}\frac{d}{dt}\mid \Phi_k\mid^2. \quad (33)$$

The system of equations (24), (26), (27), and (33) form a coupled system for the mode energy, drift velocity, and electron and ion temperature. In Appendix C, we derive the rate equation for T_e directly from Eq. (28).

If all modes have $k\lambda_D \ll 1$ and for times small enough so that v_d does not change significantly, γ_k is independent of T_i, T_e, and v_d, and it may be replaced with its initial value. Hence, $\mid E_k\mid^2$ increases exponentially with time. For times such that $T_e \gg T_e(0)$ and $T_i \gg T_i(0)$, Eqs. (33) and (26) yield

$$T_e(t) \approx (5e^2m_i^{1/2}v_d\sum_k \mid \Phi_k\mid^2)^{2/5}, \quad (34)$$

$$T_i(t) \approx \tfrac{2}{3}[T_e^{3/2}(t)/m_i^{1/2}v_d]. \quad (35)$$

Thus, the electron temperature, ion temperature, and the quantity $\sum_k \mid E_k\mid^2/k^2$ all grow exponentially with growth rates in the ratio 2:3:5. Note that the result is independent of $\langle\Delta\omega_k\rangle/\Omega_e$; it is only the magnitude of the growth rate that depends on this parameter.

One other tractable quasilinear regime is that where $k\lambda_D > 1$ for all modes. This occurs in the beam cyclotron phase if $v_e/v_d > \omega_e/\Omega_e$, since the minimum unstable value of k is Ω_e/v_d. In this regime, $\gamma_k \sim T_e^{-3/4}$ so that the coupled system no longer evolves exponentially. Combining

Eqs. (26), (33), and (24), we find that now

$$T_i(t),\ T_e(t),\ \sum_k |E_k|^2 \sim t^{4/3}, \tag{36}$$

so that the heating rate is drastically slower. Let us remark that this regime cannot occur if $\langle \Delta\omega_k \rangle \gtrsim \Omega_e/\pi$ since there is no minimum k for the ion acoustic instability.

Ion Trapping

After a period of quasilinear growth, the instability is observed to stabilize in our numerical experiments. We find experimentally, (see Sec. V) that the system stabilizes once a significant portion of the ions (typically 3–4%) become trapped. At this point, the free energy appears to dissipate by giving the ion distribution a long tail, rather than by driving exponentially growing electric fields. We will adopt the condition for the onset of ion trapping,

$$\tfrac{1}{2}m_i[v_d-(\omega_0/k_0)]^2 \approx 2e\Phi_0 \tag{37}$$

as a phenomenological condition for saturation, where k_0 is the wavenumber responsible for the trapping and Φ_0 is the amplitude of the potential fluctuation.

In order to estimate the electron temperature at saturation, we solve Eqs. (33) and (37) simultaneously for T_e. In doing so, we make one simplifying assumption, that the wave responsible for the trapping is the fastest growing mode, so that $k_0\lambda_D=(1/\sqrt{2})$ and $m_i(v_d-\omega_0/k_0)^2=\frac{2}{3}T_e$. Then, the solution for T_e at saturation is

$$T_e \approx (1/50)m_i v_d^2. \tag{38}$$

From Eq. (37) we see that $e\Phi_0/T_e \sim 0.1$. This gives $\sum_k |E_k|^2/4\pi N_0 T_e \sim 0.01$.

IV. INFLUENCE OF BEAM-CYCLOTRON INSTABILITY ON MODES WITH $kr_e \ll 1$

In the situation shown in Fig. 4, i.e., counterstreaming ion beams, and under the condition that

$$v_d/v_A < 2(1+\beta)^{1/2}$$

the beam-cyclotron instability coexists with a much slower $[\gamma_k \sim (m_e/m_i)^{1/2}\Omega_e]$ and longer wavelength $(kr_e \ll 1)$ ion–ion instability, whose theory was presented recently.[16] In the above, $v_A \equiv B/(4\pi N_0 m_i)^{1/2}$ is the Alfvén speed, and $\beta \equiv 8\pi T_e/B^2$. Since an important ingredient in the theory of this instability is the existence of magnetized electrons, the obvious question arises, whether the turbulence resulting from the beam cyclotron instability can untie the electrons from the field lines to such an extent as to render the system of Fig. 4 stable to ion–ion interaction. Physically, this would occur when the mean-square deviation of the electrons from their free orbits over the characteristic time of the instability, is of the order of the instability wavelength.

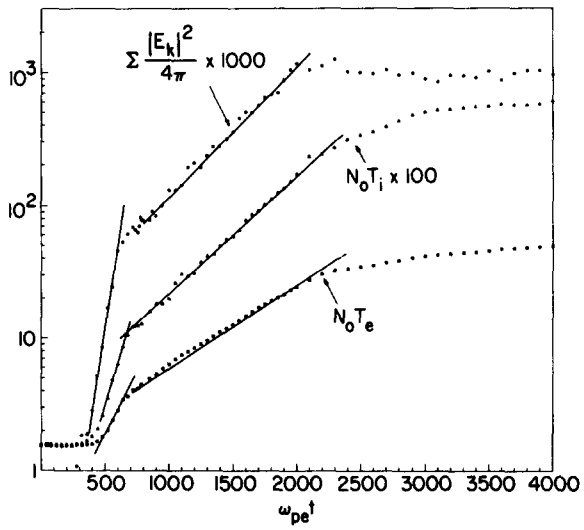

FIG. 5. Plots of electrostatic $(\Sigma |E_k|^2/4\pi)$, electron thermal (N_0T_e), and ion thermal $(\frac{1}{2}N_0T_i)$ energy densities, for run 3. Energy units are arbitrary. The solid lines are drawn to emphasize the exponential behavior during the quasilinear stages. Note that electron heating is isotropic in two dimensions because of the magnetic field, while ion heating is one-dimensional.

Using techniques similar to Sec. II, one can generalize the dispersion relation derived in Ref. 16 to include the effect of turbulent diffusion on the electrons. Assuming that the ions are cold, unmagnetized, and unaffected by the turbulent fields of the short wavelength instability the dispersion relation for propagation perpendicular to the magnetic field becomes

$$\tfrac{1}{2}[\omega_i^2/(\omega-kv_d)^2]+\tfrac{1}{2}[\omega_i^2/(\omega+kv_d)^2]=1+\mu_e^{\mathrm{NL}}, \tag{39}$$

where μ_e^{NL} is given by Eq. (15).

If

$$\gamma_i > k_i^2 D, \tag{40}$$

where γ_i and k_i are the growth rate and wavelength of the ion–ion instability,[16] then Eq. (39) reduces to the usual dispersion relation[16] in the absence of turbulent diffusion. We can therefore conclude that if condition (40) is fulfilled the short wavelength turbulence will have no effect on the ion–ion instability. In the opposite limit to (40), the diffusion term k^2D will, under some circumstances, lead to stabilization. This conclusion will be valid independently of the source of the short-wavelength turbulence, and might thus provide a mechanism of stabilizing the ion–ion system by external means.

However, in Sec. II we have seen that typically $\Delta\omega_k \equiv k^2D \sim \Omega_e$ for the case $k\lambda_D \sim 1$. Substituting k_i and γ_i for the most unstable ion–ion mode, Eq. (40) reduces to

$$(m_e/m_i)^{1/2}[(\Omega_e/\omega_e)(v_e/v_d)]^2 \ll 1,$$

a fairly weak condition. Thus the ion–ion instability is unaffected by a level of short-wavelength turbulence

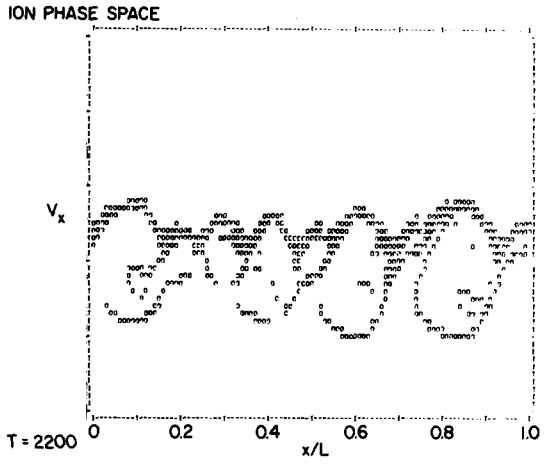

FIG. 6. Ion phase space at time $2200\,\omega_e^{-1}$. L is the system length. Note the vortex formation characteristic of trapping.

sufficient to eliminate **B** from the beam cyclotron dispersion relation. This result was confirmed by a simulation experiment to be discussed in the next section.

V. COMPUTER SIMULATION

Here, we summarize the results of nine computer experiments designed to simulate the physical system described in Sec. II. In particular, the computer code is electrostatic, with a constant magnetic field that acts on the electrons but not on the ions, in accordance with the assumption made in Sec. II. These simulation experiments confirm the main points of the theory presented in this paper. The code is the same as that used in Ref. 15; an earlier version (with no magnetic field) is described in Ref. 22.

A. Cold Ions

Table I summarizes the results of the first seven experiments.[9] Mass ratios of 400 and 1836 were used and, in all cases except one,[23] $v_d = v_e(0)$, $T_e(0) = 100T_i(0)$, the system size is 512 cells and $\lambda_D(0) = 4$ cells. Care was taken to insure that a number of unstable modes with $k\lambda_D(0) < 1$ were present in each run.

A typical graph (run 3) of field energy, electron and ion temperature versus time is shown in Fig. 5. Initially, the field energy, ion and electron temperatures all grow exponentially with growth rates in the ratio 5.5:3:1.7. This is in good agreement with the quasilinear prediction 5:3:2. Notice the drastic slowing down of the instability occurring at about $\omega_{pe}t \approx 800$. This knee is a persistent feature of all runs and marks the transition from beam cyclotron to ion acoustic instability. After the knee, the field energy, ion and electron temperatures still grow exponentially with growth rates in the ratio 3.6:3:2.1 which is in fair agreement with the quasilinear theory. At $\omega_{pe}t \approx 2200$, the instability saturates. That this saturation coincides with the onset of significant ion trapping is clearly indicated in computer printouts of phase space (see Fig. 6). The vortices shown account for about 4% of the ions. For a time of $1600\omega_{pe}^{-1}$ after saturation, the total field energy remains remarkably constant. During this time, the electron temperature increases linearly. The heating rate appears to be several times that expected from classical collisions. At this time the heating mechanism is not clearly understood and we are currently working on the late time aspects of the problem.

The theoretically predicted maximum growth rate for the beam cyclotron phase (row 7 of Table I) is in all cases larger than the observed growth rate (row 6) by a factor of about one to two. This is to be expected, since (a) it is difficult to hit the fastest growing mode since γ_k is sharply peaked, (b) other modes in the system grow more slowly, (c) numerical collisions are present, and (d) the presence of a $\langle \Delta\omega_k \rangle \sim \gamma_k < \Omega_e/\pi$ can lower the growth rate by a factor which is typically one to two [see Eq. (20)].

The theory of the transition from the beam cyclotron instability to the ordinary ion acoustic instability is well supported by the following "experimental" results. First, the level of turbulence at the knee marking this transition (see for example Fig. 5) agrees remarkably well with theory in all runs, as shown in rows 8 and 9. Second, the band structure of γ_k discussed in Sec. II is clearly observed before the knee, while γ_k becomes a smooth function of k after the knee.[9] Third, the experi-

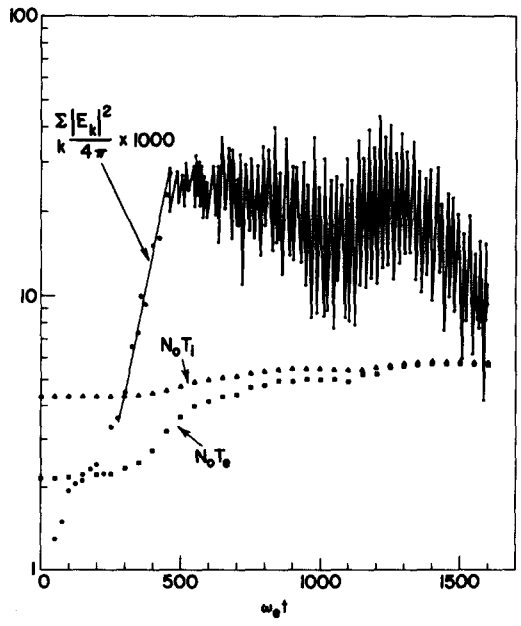

FIG. 7. Plots of electrostatic ($\Sigma |E_k|^2/4\pi$), electron thermal (N_0T_e), and ion thermal ($1/2N_0T_i$) energy densities for the case of warm ions. Energy units are arbitrary and the straight line in the early stage is to emphasize the exponential development of the fields.

mental growth rate, which agreed with the beam cyclotron growth rate before the knee, decreases markedly at the knee and agrees well with the ion-acoustic growth rate after the knee (rows 10 and 11) in all cases except the two strong magnetic field runs. In these two cases, Runs 4 and 7, the measured growth rate is smaller than the theoretical maximum ion sound growth rate by a factor of 3 to 4. This is partially accounted for by noting that $\langle\Delta\omega_k\rangle/\sqrt{2}kv_e \ll 1$ is less well satisfied for these two runs, since $\langle\Delta\omega_k\rangle$ must be rather large to smear out the electron gyroresonances. One finds that in the acoustic phase of these runs, $\langle\Delta\omega_k\rangle/\sqrt{2}kv_e$ varies from about 0.1 to 0.4. The effect of such values of $\langle\Delta\omega_k\rangle$ is to reduce the acoustic growth by a factor up to 1.5 to 2. Thus, the ion acoustic instability itself is significantly affected by the effective collision frequency $\langle\Delta\omega_k\rangle$.

B. Warm Ions

Figure 7 is a plot of electrostatic field energy, electron and ion temperatures versus time for the case $T_i(0) = 2T_e(0)$. In this run $m_i/m_e = 400$, $\omega_e/\Omega_e = 7$, the system size = 512 cells, 140 000 particles were used, $v_d = v_e(0)$ and $\lambda_D(0) = 4$ cells. Note the exponential increase in field energy at early times. This corresponds to a measured growth rate $\gamma_{m,cyc}/\omega_e = 0.006$, compared to the theoretical maximum growth rate $\gamma_{th,cyc}/\omega_e = 0.01$ for the beam cyclotron instability. At $\omega_e t \simeq 500$, the fields saturate and the instability stabilizes. This occurs at a measured turbulence level $E^2/4\pi N_0 T_e \simeq 0.009$. We attribute this stabilization to ion Landau damping at the transition from the beam cyclotron to the ion acoustic instability, since T_i/T_e is too large for unstable ion sound. The theoretical value for stabilization by this mechanism $E^2/4\pi N_0 T_e \simeq 0.009$ predicted by Eq. (23), is in excellent agreement with experiment. At stabilization the important modes have $k\lambda_D$ well below unity. Furthermore, no ion trapping is observed at stabilization. Note that over a time $1600\omega_e t$, well beyond saturation, the electron temperature has increased less than a factor of 3 and the ion temperature less than a factor of 1.5.

The level of the field energy fluctuates more after stabilization than in the case of $T_i \ll T_e$. Also there is some weaker long time heating which is not understood at present.

C. Counterstreaming Ions

We now discuss the results of a simulation performed with two equi-density ion beams counterstreaming through a Maxwellian distribution of electrons at speeds $\pm v_d$. Initially, $T_i = 10^{-2} T_e$ for both ion beams. The purpose of this experiment was to test our conclusion that a level of turbulence sufficient to eliminate the effects of the magnetic field on the scale of waves with $kr_e > 1$, will not influence fluid modes ($kr_e \ll 1$) that may be present. The choice of the two symmetrically counter-

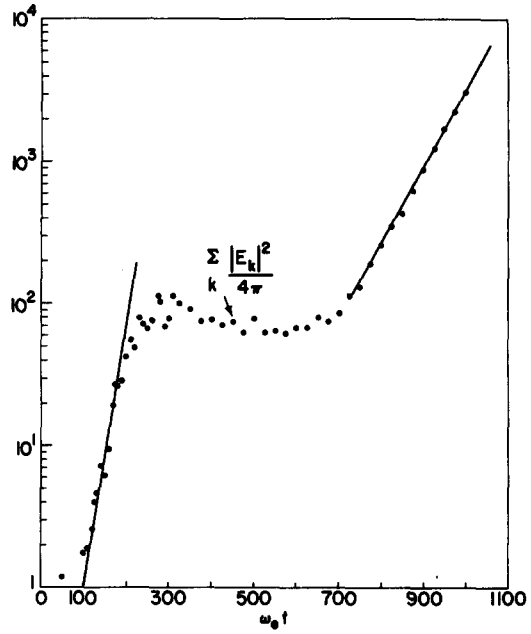

FIG. 8. Plot of electrostatic energy in arbitrary units for the case of counterstreaming ions illustrated in Fig. 3. Note the two distinct phases of exponential development (emphasized by the solid lines) corresponding to the beam cyclotron and ion-ion instabilities, respectively

streaming ion beams was made to allow the ion–ion instability discussed in Ref. 16 to be simultaneously present with the beam cyclotron instability. Since the fastest growing ion–ion mode has $\gamma_0 = \omega_0/2$ and wavenumber $k_0 = (\sqrt{3}/2)(\omega_0/v_d)$, where $\omega_0 = (\omega_i/\sqrt{2})(1+\omega_e^2/\Omega_e^2)^{-1/2}$, periodic boundary conditions $(2\pi/k)\mathfrak{N} = L$ yield

$$\mathfrak{N}_0 = (L/4\pi v_d)(3m_e/2m_i)^{1/2}[\Omega_e\omega_e/(\omega_e^2+\Omega_e^2)^{1/2}]. \quad (41)$$

Here, $\mathfrak{N}$ is the mode number, L is the system size in cells, and $\mathfrak{N}_0$ is the mode number corresponding to the fastest growing mode. Choosing parameters such that $\mathfrak{N}_0 > 1$ insures that the ion–ion instability will be present and also that the shorter wavelengths of the beam cyclotron instability will be present. Taking $L = 1024$, $\lambda_D(0) = 1$, $v_d = v_e(0)$, $m_i/m_e = 400$, $\omega_e/\Omega_e = 2$, we see from Eq. (41) that about three unstable ion–ion modes should be present. With these parameters, the theoretical growth rate for the beam cyclotron instability is approximately five times that for the ion–ion instability. In Fig. 8 we have plotted the observed electrostatic field energy as a function of time. At about $\omega_e t = 100$ the energy begins to increase exponentially with measured growth rate $\gamma_{m,cyc}/\omega_e \simeq 0.02$, compared to the theoretical maximum growth rate $\gamma_{th,cyc}/\omega_e = 0.04$ for the beam cyclotron instability. At about $\omega_e t = 250$–300 the beam cyclotron instability stabilizes at a level of turbulence $|E|^2/4\pi N_0 T_e \simeq 0.08$ which is just below the level $|E|^2/4\pi N_0 T_e \simeq 0.1$ predicted by Eq. (23) for the transition to the usual ion acoustic instability. At this point two nonlinear effects suppress the ion acoustic instability: $k_{min}\lambda_D = (\Omega_e/\omega_e)(v_e/v_d) \approx 1$ and

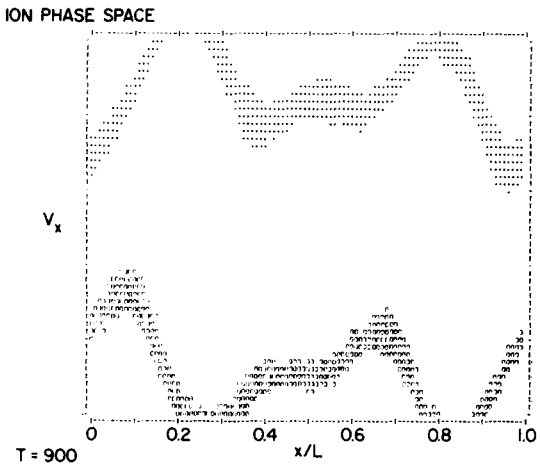

FIG. 9. Ion phase space for the counterstreaming ion simulation at time 900 ω_e^{-1}. Note the clear evidence of the long wavelength ion–ion instability.

also the fields are large enough to trap the ions. After the saturation the total field energy remains relatively steady while the unstable ion–ion modes grow. At about $\omega_e t = 700$, these modes rise above the fluctuation level of the saturated beam cyclotron instability and the subsequent exponential increase in the total electrostatic energy is due to the ion–ion instability.

The measured growth rate $\gamma_{m,I-I}/\omega_e \simeq 0.006$ agrees very well with the maximum theoretical growth rate $\gamma_{th,I-I}/\omega_e \simeq 0.008$. Computer printouts of ion phase space plots clearly indicate the presence of a strong ion–ion instability at these later times (see Fig. 9). Furthermore, plots of mode amplitude versus k clearly show that the short wavelengths of the beam cyclotron instability dominate in the early stage, whereas the long wavelengths of the ion–ion instability dominate the later stage. Thus, we confirm the prediction that a level of turbulence strong enough to smear out the electron gyroresonances on modes $kr_e > 1$ will have virtually no effect on fluid modes with $kr_e \ll 1$.

VI. CONCLUSION

Our main conclusion from the analysis and computer results presented here is that short wavelength $\lambda \sim \lambda_D$ electrostatic turbulence is insensitive to the presence of a static magnetic field, after the early stages of development, provided ω_e^2/Ω_e^2 is a reasonably large number. This is an important point to keep in mind in the treatment of (i) turbulent heating experiments involving current flow across magnetic field lines and (ii) cross-field collisionless shock waves. In these situations the magnetic fields may be playing no role other than preventing the electrons from being trapped in the potential troughs of the waves, since it is clear that an electron cannot be trapped in a wave indefinitely, in the presence of a static magnetic field normal to the wave.

Thus, we expect that the structure of the cross-field shock wave in the experiments of Refs. 12 and 24, where $T_i \ll T_e$ is determined primarily by the properties of ordinary ion acoustic instability. In the experiment reported by Keilhacker and Steuer[11] $T_i \sim T_e$, and the beam cyclotron modes are linearly unstable. However, the turbulence level necessary for the transition from beam-cyclotron to ion-acoustic turbulence is quite low since $\omega_e/\Omega_e \gg 1$, and, in fact, is much less than the experimentally measured value. If the ions are Maxwellian, then ion acoustic waves are stable for $T_i \sim T_e$, but this is not necessarily true if a sizeable fraction of the ion energy resides in a non-Maxwellian tail. This matter is presently being investigated.

Finally, we have shown that the long wavelength portion of the turbulent spectrum may be relatively unaffected by the diffusion caused by short wavelengths provided $\Delta\omega_k \equiv k^2 D \ll \gamma_k$ where k and γ_k pertain to the long wavelength.

ACKNOWLEDGMENT

The work of one of us (K. P.) was supported in part by National Aeronautics and Space Administration Grant NGL-21-002-005.

APPENDIX A

In this appendix we outline the derivation of Eq. (4) for μ_e following the procedure of Ref. 17. Using the identity

$$\oint_C \frac{d\nu}{\sin\pi\nu} \frac{J_\nu(z)J_{-\nu}(z)}{\nu-\alpha} = 0, \tag{A1}$$

where C is a circular contour with radius $R \to \infty$, it follows that

$$\sum_{n=-\infty}^{\infty} \frac{J_n^2(z)}{\alpha-n} = \frac{\pi J_\alpha(z)J_{-\alpha}(z)}{\sin\pi\alpha}. \tag{A2}$$

Thus, Eq. (3), for a Maxwellian distribution of electrons may be written as

$$\mu_e = (k^2\lambda_D^2)^{-1}\left[1 - \frac{\pi\tilde{\omega}}{v_e^2 \sin\pi\tilde{\omega}} \times \int_0^\infty dv_\perp\, v_\perp J_{\tilde{\omega}} J_{-\tilde{\omega}} \exp\left(-\frac{v_\perp^2}{2v_e^2}\right)\right], \tag{A3}$$

where $\tilde{\omega} \equiv \omega/\Omega_e$. Using the following integral relations:

$$J_\alpha(z)J_{-\alpha}(z) = \frac{2}{\pi}\int_0^{\pi/2} d\theta \cos(2\alpha\theta) J_0(2z\cos\theta) \tag{A4}$$

and

$$\int_0^\infty J_0(bt)\exp(-p^2t^2)t\,dt = \frac{1}{2p^2}\exp\left(-\frac{b^2}{4p^2}\right), \tag{A5}$$

Eq. (A3) becomes

$$\mu_e=(k^2\lambda_D^2)^{-1}\left[1-\frac{2\tilde{\omega}}{\sin\pi\tilde{\omega}}\int_0^{\pi/2}d\phi\cos[2\tilde{\omega}(\tfrac{1}{2}\pi-\phi)]\right.$$
$$\left.\times\exp\left(-\frac{2k^2v_e^2}{\Omega_e^2}\sin^2\phi\right)\right], \quad \text{(A6)}$$

with $\phi=\frac{1}{2}\pi-\theta$.

For $kv_e/\Omega_e>1$ most of the contribution to the integral in Eq. (A6) comes from ϕ small. Therefore, we may approximate the integral by removing the upper limit to infinity and replacing $\sin^2\phi$ in the exponential factor with ϕ^2. Writing the cosine term in exponential form, the resulting integrals are then in the form of plasma dispersion functions, and Eq. (4) follows.

APPENDIX B

For the case of cold ions, the beam cyclotron instability is a "quantized" version of the usual ion sound instability. The magnetic field deforms the continuous instability spectrum into discrete bands of instability, without mixing the unstable branch of the ion sound spectrum with any damped branch. This fact is tied up with a rather remarkable theorem which is proven in this Appendix: If $T_i=0$, the quantity

$$Q\equiv\int_{-\infty}^{\infty}dk\,\gamma_k, \quad \text{(B1)}$$

where the integral is taken *over the unstable modes only* (i.e., $\gamma_k>0$), is independent of the magnetic field. In particular, Q has the same value for the beam-cyclotron instability as for the ion-acoustic instability.

This theorem should be applicable to certain other magnetic instabilities, as will be seen from the proof. However, for the beam cyclotron instability with hot ions, the unstable modes do not form a branch distinct from the Landau damped modes, and the theorem fails.

The outline of the proof is as follows. For $T_i=0$, the dispersion relation is

$$D(k,\omega)\equiv 1-\frac{\omega_i^2}{(\omega-kv_d)^2}-(k^2\lambda_D^2)^{-1}$$
$$\times\sum_{n=-\infty}^{\infty}\exp(-k^2r_e^2)I_n(k^2r_e^2)\frac{n\Omega_e}{\omega-n\Omega_e}=0. \quad \text{(B2)}$$

Since the zeros of D are $\omega_k^{\pm}=\omega_k\pm i\gamma_k$, Eq. (B1) can be written

$$Q=\int_{-\infty}^{\infty}dk\,\mathrm{Im}(2\pi i)^{-1}\int_C d\omega\,\omega D^{-1}\frac{\partial D}{\partial\omega}, \quad \text{(B3)}$$

where C is the contour shown in Fig. 2, enclosing all roots of Eq. (B2) with $\gamma_k>0$. The semicircle at infinity does not contribute, since the integrand $(\omega/D)(\partial D/\partial\omega)\sim\omega^{-2}$ as $|\omega|\to\infty$. The order of integration is now reversed, giving

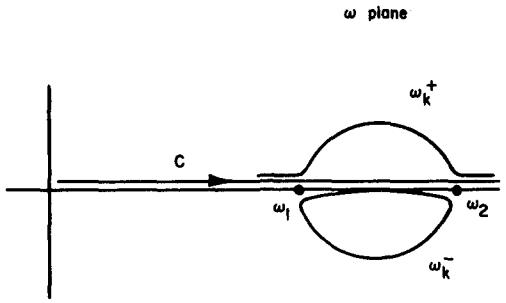

FIG. 10. Path traced out by $\omega_k^{\pm}$ in the ω plane as k varies in the vicinity of an instability band.

$$Q=\mathrm{Im}(2\pi i)^{-1}\int_{-\infty+i\delta}^{\infty+i\delta}d\omega\,\omega\int_{-\infty}^{\infty}dk\,D^{-1}\frac{\partial D}{\partial\omega}. \quad \text{(B4)}$$

If it can be shown that

$$\int_{-\infty}^{\infty}\frac{dk}{D}\frac{\partial D}{\partial\omega}$$

is an analytic function of ω in the upper half ω plane, then the ω contour in (B4) can be moved up to $i\infty$. But as $\mathrm{Im}\omega\to\infty$, $D^{-1}(\partial D/\partial\omega)$ becomes independent of B. Thus, Q is independent of B.

We now discuss some subtleties in the proof. Note first that $D(k,\omega)=D(-k,-\omega)$, and that D is real for real k and real ω. It follows that if $D(k,\omega)=0$, then $D(-k,-\omega^*)=0$. As a result of this symmetry (which is convenient but not essential to the proof), Eq. (B3) can be simplified to

$$Q=(2\pi i)^{-1}\int_{-\infty}^{\infty}dk\int_C d\omega\,\omega D^{-1}\frac{\partial D}{\partial\omega}. \quad \text{(B5)}$$

For k real, the integrand of Eq. (B5), $(\omega/D)\partial D/\partial\omega$, has an infinite set of poles on the real ω axis (two near each cyclotron harmonic $\omega=n\Omega_e$). These poles contribute nothing to Q and are of no interest. In addition, if k happens to fall in a band of instability, $(\omega/D)\partial D/\partial\omega$ also has a pair of first-order poles $\omega_k^{\pm}\equiv\omega_k\pm i\gamma_k$ at conjugate complex values of ω (see Fig. 1, and note that another branch of modes with $\gamma_k<0$ is given by reflecting the curve in the horizontal k axis.) The single pole ω_k^+ in the upper half ω plane is the only one that contributes to Q.

A difficulty ensues from the fact that as k approaches the extrema of an instability band, $\gamma_k\to 0$ (see Fig. 1), so that the two conjugate poles ω_k^+ and ω_k^- meet on the real ω axis, pinching the contour C between them. This corresponds to a branch point of the function

$$F(k)\equiv\int_{-\infty+i\delta}^{\infty+i\delta}d\omega\frac{\omega}{D}\frac{\partial D}{\partial\omega}$$

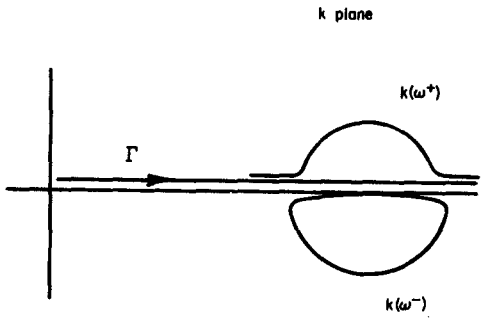

FIG. 11. Path traced out by values of k corresponding to the roots $\omega_k^{\pm}$.

on the real k axis, for each value of k which begins or ends an instability band. To avoid this difficulty, we rewrite Q as

$$Q=\int_{-\infty+i\epsilon}^{\infty+i\epsilon} dk\gamma_k=\int_{C-\infty+i\epsilon}^{\infty+i\epsilon} dk\int_{\Gamma-\infty+i\delta}^{\infty+i\delta} d\omega\,\frac{\omega}{D}\frac{\partial D}{\partial\omega}. \quad \text{(B6)}$$

Since γ_k is a continuous function of k, it is clear that adding the infinitesimal $i\epsilon$ to k does not change Q.

We now consider the path traced out in the ω plane by the roots $\omega_k^{\pm}$, as k varies on the upper real k axis. The topology of this path can be seen from the approximate solution, Eqs. (8), which can be written (omitting inessential correction terms) as

$$\omega_k^{\pm}=\tfrac{1}{2}k(v_d-c_s)+\tfrac{1}{2}n\Omega_e\pm\{[k(v_d-c_s)-n\Omega_e]^2 - (m_e/8\pi m_i)^{1/2}n\Omega_e^2\}^{1/2}. \quad \text{(B7)}$$

The path traced out by $\omega_k^{\pm}$ in the ω plane as k varies on the upper real axis in the vicinity of an instability band, according to Eq. (B7), is shown in Fig. 10. If k were allowed to become real, the two branches would converge and pinch at the points ω_1 and ω_2. But as long as $\epsilon>0$ in Eq. (8), δ can be chosen so that the ω contour C splits the two branches (and also runs above all the uninteresting singularities strung out nearly on the real ω axis.)

The order of integration can now be reversed, since the integrand is well behaved on the contour of integration. This gives

$$Q=\int_{C-\infty+i\delta}^{\infty+i\delta} d\omega\,\omega G(\omega), \quad \text{(B8)}$$

where the function $G(\omega)$ is defined, for ω on the contour C, by

$$G(\omega)=\int_{\Gamma-\infty+i\epsilon}^{\infty+i\epsilon} dk\,D^{-1}\frac{\partial D}{\partial\omega}. \quad \text{(B9)}$$

It can be seen, by solving Eq. (B7) for k, that as ω varies over C, the values of k corresponding to the roots $\omega_k^{\pm}$ trace out a path in the k plane shown in Fig. 11. [The solutions $k(\omega^{\pm})$ are of the same form as $\omega_k^{\pm}$; thus, Fig. 11 is of the same nature as Fig. 10.] The k contour Γ splits the two branches. The various uninteresting singularities lie either slightly above or slightly below Γ.

$G(\omega)$ can be analytically continued into the upper half ω plane by the definition (B9), with the proviso that if any singularity of $[1/D(k,\omega)]\partial D/\partial\omega$ tries to cross the contour Γ as ω varies, then Γ is distorted so as to prevent this. If this is possible, then $G(\omega)$ is analytic in the entire upper half ω plane. A difficulty could arise only if Γ is pinched between two converging singularities. But we have seen that the singularities ω_k^{+} and ω_k^{-} cannot meet except at a real value of k (and, in fact, no two singularities of $(1/D)\partial D/\partial\omega$ can converge on Γ).

Since G is analytic, the ω contour C in Eq. (B8) can be pushed up to $i\infty$, i.e., we let $\delta\to\infty$. But for $\mathrm{Im}\omega\to\infty$, D becomes independent of B. This can be proven most easily from the identity

$$\sum_{n=-\infty}^{\infty}\frac{n\Omega_e\exp(-k^2v_e^2/\Omega_e^2)I_n(k^2v_e^2/\Omega_e^2)}{\omega-n\Omega_e} = \frac{k^2v_e^2}{\Omega_e^2}\int_0^{\infty}d\tau\sin(\Omega_e\tau)\exp\left[i\omega\tau-\frac{k^2v_e^2}{\Omega_e^2}(1-\cos\Omega_e\tau)\right]. \quad \text{(B10)}$$

As $\mathrm{Im}\omega\to\infty$, the right-hand side of Eq. (B10) goes to $-k^2v_e^2/\omega^2$. Thus, Q is independent of B which completes the proof.

Finally, we note that if $T_i\neq 0$, then roots $\omega_k+i\gamma_k$ no longer come in complex conjugate pairs. If we follow the path traced out in the ω plane by an unstable root $\omega_k+i\gamma_k$, as k varies, then we find that $\omega_k+i\gamma_k$ crosses the real ω axis and becomes damped for values of k below some critical value.[8] This invalidates our theorem as stated, although the theorem is, of course, still approximately true if $T_i\ll T_e$.

APPENDIX C

In this appendix we evaluate the rate of change of electron energy directly from the quasilinear equation. The electron quasilinear equation may be written as

$$\frac{\partial f_e}{\partial t}=\mathrm{Re}\sum_k\frac{2e}{m_e}\frac{\partial}{\partial\mathbf{v}}\cdot\langle\mathbf{E}_{-k}f_{ke}\rangle, \quad \text{(C1)}$$

where the summation is over positive k. The above expression for $\partial f_e/\partial t$ can be computed from the equation for f_{ke} including resonance broadening. This can be obtained from Eqs. (37), (39), and (59) of Ref. 14. The result is

$$\frac{\partial f_e}{\partial t}=-\frac{2e^2}{m_e^2}\mathrm{Im}\sum_k\sum_n\frac{n\Omega_e}{v_\perp}\frac{\partial}{\partial v_\perp}\frac{J_n^2\,|\,\Phi_k\,|^2}{\langle\bar{\omega}_k\rangle-n}\frac{\omega}{v_\perp}\frac{\partial f_e}{\partial v_\perp}, \quad \text{(C2)}$$

where $\langle\bar{\omega}_k\rangle\equiv(\omega+i\langle\Delta\omega_k\rangle)/\Omega_e$. If $\langle\Delta\omega_k\rangle=0$, Eq. (C2)

reduces to the standard form since $(\omega/v_\perp)\,\partial f_e/\partial v_\perp$ may be replaced by $(n\Omega_e/v_\perp)\,\partial f_e/\partial v_\perp$. Note, however that a nonzero value of $\langle\Delta\omega_k\rangle$ alters the *form* of the usual quasilinear equation and that it is not enough to simply replace γ_k by $\gamma_k+\langle\Delta\omega_k\rangle$. Taking the appropriate moment of Eq. (C2) and employing the techniques used in Appendix A, we obtain

$$\frac{dT_e}{dt}=\frac{2e^2}{T_e}\sum_k |\Phi_k|^2\,\mathrm{Im}\{\omega[1+\tfrac{1}{2}\zeta(Z(\zeta)-Z(-\zeta)+i\cot(\pi\langle\bar{\omega}_k\rangle)[Z(\zeta)+Z(-\zeta)])]\},\quad \text{(C3)}$$

where $\zeta\equiv(\omega+i\langle\Delta\omega_k\rangle)/\sqrt{2}kv_e$.

For $c_s<v_d<v_e$, and $T_i\ll T_e$, it is now easy to show that Eq. (C3) reduces to Eq. (33) in either of the limits (i) $\langle\Delta\omega_k\rangle$, γ_k, $\omega_k-n\Omega_e\ll\Omega_e/\pi$, or (ii) $\langle\Delta\omega_k\rangle\gtrsim\Omega_e/\pi$.

* On leave of absence from Cornell University, Ithaca, New York.

[1] O. Buneman, J. Nucl, Energy, Pt. **C4,** 111 (1961).
[2] R. Z. Sagdeev, in *Advances in Plasma Physics*, edited by M. A. Leontovich, (Consultants Bureau, New York, 1966), Vol. 4, p. 23.
[3] N. A. Krall and D. L. Book, Phys. Fluids **12,** 347 (1969).
[4] H. V. Wong, Phys. Fluids **13,** 757 (1970).
[5] S. P. Gary and J. J. Sanderson, J. Plasma Phys. **4,** 739 (1970).
[6] C. N. Lashmore-Davies, J. Phys. **A3,** L40-45 (1970).
[7] D. W. Forslund, R. L. Morse, and C. W. Nielson, Phys. Rev. Letters **25,** 1266 (1970).
[8] M. Lampe, J. B. McBride, J. H. Orens, and R. N. Sudan, Phys. Letters **35A,** 131 (1971).
[9] M. Lampe, W. M. Manheimer, J. B. McBride, J. H. Orens, R. Shanny, and R. N. Sudan, Phys. Rev. Letters **26,** 1221 (1971).
[10] W. D. Davis, A. W. DeSilva, W. F. Dove, H. R. Griem, N. A. Krall, and P. C. Liewer, Presented at the Conference on Plasma Physics and Controlled Nuclear Fusion Research, Madison, Wisconsin (1971); N. A. Krall and P. C. Liewer, Phys. Rev. Letters (to be published).
[11] M. Keilhacker and K. H. Steuer, Phys. Rev. Letters **26,** 694 (1971).
[12] S. P. Gary and J. W. M. Paul, Phys. Rev. Letters **26,** 1097 (1971); P. Bogen, K. J. Dietz, K. H. Dippel, E. Hintz, K. Höthker, F. Siemson, and G. Zeyer, Presented at the Conference on Plasma Physics and Controlled Fusion Research, Madison, Wisconsin (1971).
[13] The electron current due to the $\mathbf{E}\times\mathbf{B}$ drift must be larger than the sum of the diamagnetic current and the electron current arising from the grad B drift. The reason is that the former current is parallel to curl $\mathbf{B}$, while the latter two currents are antiparallel. See J. B. McBride, W. M. Manheimer, and M. Lampe (to be published).
[14] C. T. Dum and T. H. Dupree, Phys. Fluids **13,** 2064 (1970).
[15] It should be recognized that ion trapping, when many waves are involved, is of the same nature as gyroresonance broadening discussed in Sec. IIB. However, for the situations discussed in this paper, ion trapping/resonance broadening occurs at a higher level of turbulence.
[16] K. Papadopoulos, R. C. Davidson, J. M. Dawson, I. Haber, D. A. Hammer, N. A. Krall, and R. Shanny, Phys. Fluids **14,** 849 (1971).
[17] B. Coppi, M. N. Rosenbluth, and R. N. Sudan, Ann. Phys., (N.Y.) **55,** 207 (1969).
[18] Here and in what follows, we specialize the discussion to $\mathbf{k}\,||\,\mathbf{v}_d$. To obtain the results for $\mathbf{k}$ normal to $\mathbf{B}$ but at an arbitrary angle ϕ to $\mathbf{v}_d$, replace v_d by $v_d\cos\phi$.
[19] T. H. Dupree, Phys. Fluids **9,** 1733 (1966).
[20] This result was taken from T. E. Stringer, J. Nucl. Energy, Pt. **C6,** 267 (1964).
[21] C. T. Dum and R. N. Sudan, Phys. Rev. Letters **23,** 1149 (1969).
[22] J. M. Dawson, C. G. Hsi, and R. Shanny in *Plasma Physics and Controlled Nuclear Fusion Research* (International Atomic Energy Agency, Vienna, 1969), Vol. 1, p. 735.
[23] In run 2 we took $v_d=0.8\ v_e$ (0), $\lambda_D(0)=5$, $T_e(0)=100\times T_i(0)$ and the system length $=1024$ cells.
[24] J. W. M. Paul, C. C. Daughney, and L. S. Holmes, Nature **223,** 822 (1969).